Struct Multidisc Optim
DOI 10.1007/s00158-012-0845-x

INDUSTRIAL APPLICATION

Process for design optimization of honeycomb core sandwich panels for blast load mitigation

S. K. Nayak · A. K. Singh · A. D. Belegundu · C. F. Yen

Received: 25 February 2012 / Revised: 14 August 2012 / Accepted: 15 August 2012

Abstract A general process for optimization of a sandwich panel to minimize the effects of air blast loading is presented here. The panel geometry consists of two metal face plates with a crushable honeycomb or other type of core. Optimization is necessary as there is strong coupling between the several variables and the physics, which makes parametric studies relatively ineffective. Virtual testing is used to develop a homogenized model for the stress–strain curve of the honeycomb core, which can be readily applied to other types of cellular core. The homogenized model has been validated by comparison to existing results as well as to results from detailed finite element (FE) models. A design of experiments (DOE) based response surface optimization method in combination with LS-DYNA is used to minimize dynamic deflection or acceleration of the back face plate. Constraints on total mass and on plastic strain in the face plates are imposed. The mechanism of lowering the backface deflection is by increasing front face plate thickness which effectively distributes the blast load to a larger area of the core and avoids local concave deformation of the front face plate. Further, core depth is increased which increases panel stiffness. For acceleration minimization, results again produce a stiffer front face plate, but accompanied by a sufficiently soft core. The mechanism of lowering the backface acceleration is by absorbing energy with low transmitted stress. A clear cut comparison between monolithic metal plates and sandwich plates, for the same loading and failure criteria, is presented here.

Keywords Honeycomb · Homogenization · Blast · Optimization · Sandwich plates · Virtual testing

1 Introduction

Sandwich panels, such as a honeycomb core with two metal facing plates, are finding increasing use over monolithic or solid plates in structural design to withstand intense short duration pressure loads. Applications include protection of land vehicles, ships or other structures. The cellular core has the ability to absorb the impact energy of the pressure pulse by undergoing large plastic deformation at almost constant nominal stress. This characteristic of the cellular core results in significant reduction in the backface acceleration and hence mitigates the damage causing potential of the blast impulse. Though metal sandwich panels have been used for a long time in aircraft and other light weight structures to maximize the bending stiffness per unit density, only recently have researchers investigated the possible use of sandwich panels for blast protection. In sandwich panels, studies involving one or at most two parameters at-a-time have been carried out. However, optimization with several variables is necessary to capture interacting physics which include: (1) too thin a front face plate will result in significant concave deformation under load that will increase the momentum on the structure which is detrimental, (2)

S. K. Nayak · A. K. Singh
The Pennsylvania State University, University Park, PA, USA

S. K. Nayak
Brookhaven National Laboratory, Upton, NY, USA

A. D. Belegundu (✉)
Mechanical and Nuclear Engineering, The Pennsylvania State University, University Park, PA, USA
e-mail: adb3@psu.edu

C. F. Yen
Army Research Laboratory - WRMD,
Aberdeen Proving Ground, MD, USA

Published online: 09 November 2012

Report Documentation Page

Form Approved
OMB No. 0704-0188

1. REPORT DATE	2. REPORT TYPE	3. DATES COVERED
2012		**00-00-2012 to 00-00-2012**

4. TITLE AND SUBTITLE	5a. CONTRACT NUMBER
Process for design optimization of honeycomb core sandwich panels for blast load mitigation	5b. GRANT NUMBER
	5c. PROGRAM ELEMENT NUMBER
6. AUTHOR(S)	5d. PROJECT NUMBER
	5e. TASK NUMBER
	5f. WORK UNIT NUMBER
7. PERFORMING ORGANIZATION NAME(S) AND ADDRESS(ES) **Army Research Laboratory - WRMD,Aberdeen Proving Ground,MD,20783**	8. PERFORMING ORGANIZATION REPORT NUMBER
9. SPONSORING/MONITORING AGENCY NAME(S) AND ADDRESS(ES)	10. SPONSOR/MONITOR'S ACRONYM(S)
	11. SPONSOR/MONITOR'S REPORT NUMBER(S)

12. DISTRIBUTION/AVAILABILITY STATEMENT
Approved for public release; distribution unlimited

13. SUPPLEMENTARY NOTES
Structural and Multidisciplinary, Optimization, vol 46, no. 6, December 2012

14. ABSTRACT

A general process for optimization of a sandwich panel tominimize the effects of air blast loading is presented here. The panel geometry consists of two metal face plates with a crushable honeycomb or other type of core. Optimization is necessary as there is strong coupling between the several variables and the physics, which makes parametric studies relatively ineffective. Virtual testing is used to develop a homogenized model for the stress?strain curve of the honeycomb core, which can be readily applied to other types of cellular core. The homogenized model has been validated by comparison to existing results as well as to results from detailed finite element (FE) models. A design of experiments (DOE) based response surface optimization method in combination with LS-DYNA is used to minimize dynamic deflection or acceleration of the back face plate. Constraints on total mass and on plastic strain in the face plates are imposed. The mechanism of lowering the backface deflection is by increasing front face plate thickness which effectively distributes the blast load to a larger area of the core and avoids local concave deformation of the front face plate. Further, core depth is increased which increases panel stiffness. For acceleration minimization results again produce a stiffer front face plate, but accompanied by a sufficiently soft core. The mechanism of lowering the backface acceleration is by absorbing energy with low transmitted stress. A clear cut comparison between monolithic metal plates and sandwich plates, for the same loading and failure criteria, is presented here.

15. SUBJECT TERMS

16. SECURITY CLASSIFICATION OF:			17. LIMITATION OF ABSTRACT	18. NUMBER OF PAGES	19a. NAME OF RESPONSIBLE PERSON
a. REPORT	b. ABSTRACT	c. THIS PAGE			
unclassified	**unclassified**	**unclassified**	**Same as Report (SAR)**	**16**	

front and back face plate thicknesses must ensure proper load transfer to the core to enable crushing, (3) the core itself must be stiff enough to minimize peak backface displacement and soft enough to crush and absorb energy to minimize acceleration, (4) total mass and space or envelope constraints must be satisfied, and (5) face plates must be thick enough to maintain integrity.

In this paper, a process is presented which enables simultaneous consideration of several variables relating to core and face plate geometry. A key step in the process is a validated approach to generating a homogenized model for the honeycomb core. A design of experiments (DOE) based response surface optimization method in combination with LS-DYNA is used to minimize dynamic deflection or acceleration of the back face plate. Constraints on mass and on plastic strain in the face plates are imposed. Further, a clear cut comparison between monolithic metal plates and sandwich plates for the same loading and failure criteria is presented here.

The shape of a monolithic aluminum plate to reduce dynamic displacement under blast was optimized in Argod et al. (2010) and Belegundu et al. (2008). For this, a differential evolution optimizer was coupled to LS-DYNA to minimize the plate's peak displacement subject to limits on mass and on peak plastic strain; the shaped plate performed very well compared to a flat plate of equal mass. Xue and Hutchinson (2004) compared the performance of sandwich panels (such as pyramidal truss core, square honeycomb and folded plate) to a monolithic plate of equal weight for blast resistance. They found that square honeycomb and folded plate outperformed the pyramidal truss core, but all three sandwich panels were capable of offering higher blast resistance compared to the monolithic plate. Their optimization study did not consider material failure, shape and certain core parameters. Fleck and Deshpande (2004) developed an analytical methodology to analyze the dynamic response of metallic sandwich beams subject to both air and water blasts. Their finding on the basis of simple analytical formulas matched well with the result from Xue and Hutchinson's (2004) three-dimensional FE calculations. Yen et al. (2005) carried out both experimental and computational analyses to study the effect of honeycomb crush strength on the dynamic response of a honeycomb core sandwich pendulum system. The result indicated that total impulse of the system increased due to concave deformation of the front face plate, and that significant reduction in maximum stress amplitude propagating within the core can be achieved by suitable selection of honeycomb material with proper crush strength. Further, suitable shape of the front face plate can reduce the concave deformation and hence the total blast impulse. Numerical analyses carried out in LS-DYNA using ConWep air blast function validated the experimental result. Hanssen et al. (2002) performed similar tests on aluminum foam core sandwich panels with similar results. Main and Gazonas (2008) investigated the uniaxial crushing of a cellular sandwich plate subjected to air blast. The study showed that the shock transmission can be reduced by suitably distributing the mass among the face plates and the core for a given mass of the sandwich. The study considered the effect of face plate thicknesses and core depth but did not consider parameters related to the core such as core density. They showed that prior to densification, the core provides structural support to the front plate and regulates the stress transferred to the back face plate. Once the onset of core densification starts, higher stresses are transferred to the back face plate (Main and Gazonas 2008; Chi et al. 2010). Zhu et al. (2008, 2009) presented a limited optimal design study of the honeycomb sandwich panel and showed that there exists an optimum core density and core depth to minimize the sandwich deflection. Karagiozova et al. (2009) states that the optimum sandwich configuration depends upon the applied blast load, and an optimum structure compromises between energy absorption of the core and the load transfer to the back face plate of sandwich. For the same load, the acceleration of the back face plate also depends upon the mass of the back face plate.

It is relevant to also cite papers that address the stress–strain response of honeycomb sandwich panels, as these have helped to validate portions of the homogenization process in this paper. Yamashita and Gotoh (2005) studied the impact behavior of honeycomb cells through numerical simulations and experiments. Numerical simulation using a single 'Y' cross-sectional unit cell model predicted the crush behavior quite well compared to experiments with drop hammer velocity of 10 m/s. Highest crush strength per unit mass was obtained when cell shape is a regular hexagon. Wierzbicki (1983) derived a simple formula from the basic principles of material continuity and plasticity for calculating the mean crush strength of metal honeycombs in terms of the cell diameter, foil thickness and the flow stress. The derivation is given for a general shape, and is then specified for a regular hexagon cell. The result from this analytical solution is well matched to the experimental results. Zhang and Ashby (1992) analyzed the collapse behavior of the honeycomb under both axial compression and in-plane shear load. Buckling, debonding and fracture are identified as possible collapse mechanisms. For flexible honeycombs such as those made from Nomex, buckling and fracture are dominant mode of failure in simple axial compression test, but for rigid-plastic honeycombs (made from aluminum), buckling and plastic yielding dominates. Depth of the honeycomb has no effect and cell angle has little effect on out-of-plane strengths (compressive and shear). These strengths are highly sensitive to the density of the honeycomb. It is also found that out-of-plane loading has

little effect on in-plane failure and vice versa. Wu and Jiang (1997) performed both quasi-static and high speed impact (up to 28.14 m/s) crush test on six types honeycomb cellular structure. They mentioned that small cell size, short height honeycomb made from high strength material has high energy absorbing capacity.

2 Homogenization of honeycomb structure via nonlinear virtual testing

It is necessary to homogenize the honeycomb core, as a detailed finite element model of a sandwich panel with a core will require a high density mesh to capture the cyclic plastic buckling or 'folding' deformation of the core accurately, entailing enormous computing time for each analysis. Moreover, optimization involves iterative analysis. Homogenization will allow the honeycomb to be replaced by a 3-D continuum structure which can then be modeled using, say, eight-noded hexahedral elements. A process is given here which can be used to homogenize any structural concept for the core. The main steps are: (1) a unit cell is identified and a FE model of the cell is developed, (2) geometrical parameters associated with the unit cell are identified, (3) nonlinear virtual testing is carried out for different values of the geometrical parameters, followed by curve fitting which parametrizes the stress–strain curve in terms of the geometrical parameters, (4) validation of the homogenized model both by detailed FE modeling of the unit cell and/or of a test specimen and by comparison to any existing results in the literature. Since the actual blast panel undergoes compression as well as bending, validation must include different types of virtual tests. Following this, optimization of the geometry of both the honeycomb core and of the face plates is carried out. These four steps are described below.

2.1 Unit cell

Figure 1 shows the hexagonal cell structure, its unit cell, and its FE model. The simplest repeating unit in this structure is a 'Y' shape, which is taken to be the unit cell (Yamashita and Gotoh 2005). The regular hexagon cell, branch angle = 120°, is considered here as it gives the highest crush strength per unit mass (Yamashita and Gotoh 2005). The unit cell

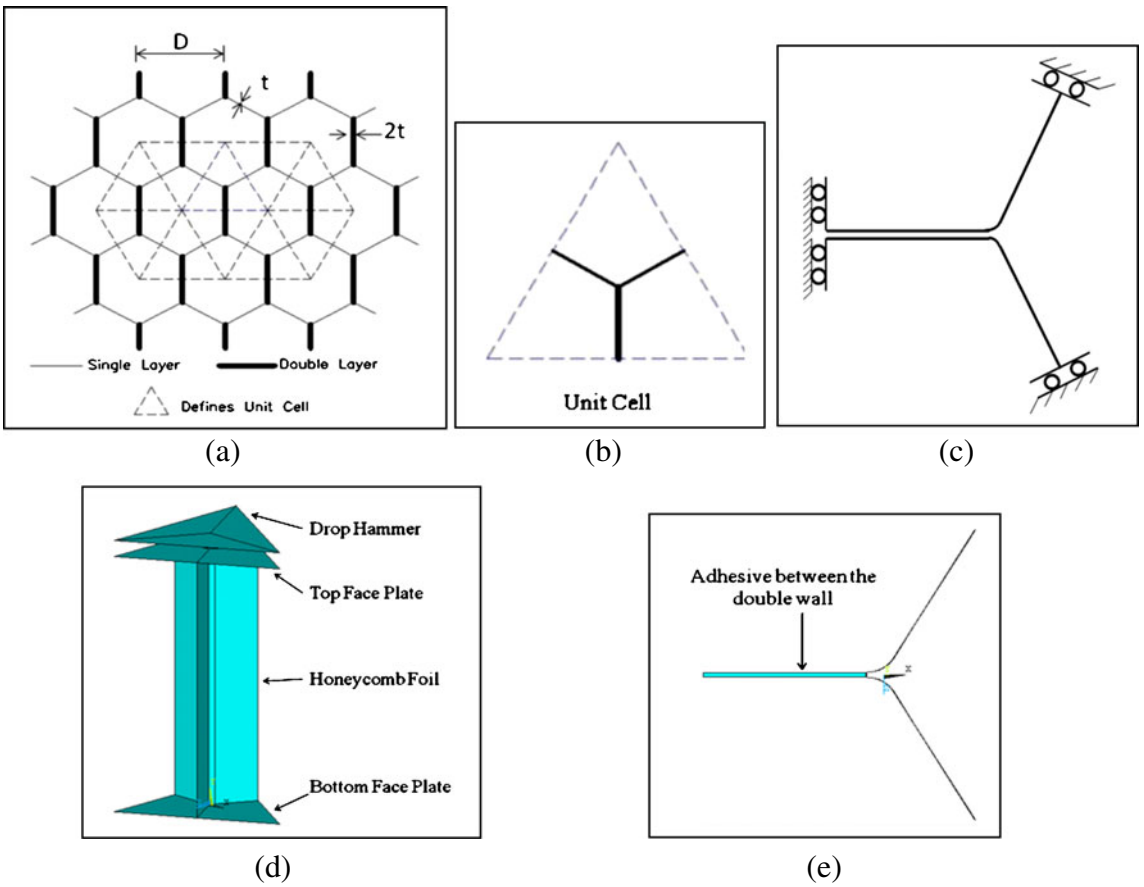

Fig. 1 Numerical model of honeycomb core (**a**) Honeycomb cell geometry, (**b**) Unit cell, (**c**) Boundary conditions on the unit cell, (**d**) FEM in LSDYNA and (**e**) Adhesive in model

Table 1 Material properties of the honeycomb unit cell model

Material	Density (kg/m^3)	Young's modulus (GPa)	Yield Stress (MPa)	Tangent modulus (MPa)	Poison's ratio
Foil-AL5052	2680	72	300	50	0.34
Adhesive	2000	5	30	0	0.3
Drop Hammer-Steel	288×10^5	200	–	–	0.24

has one double wall and two single walls. The double wall consists of two layers of foil glued together by an adhesive. LS-DYNA is used to carry out the virtual simulation. The foil is modeled by quadrilateral Belytschko-Tsay shell elements, and the 0.01 mm thick layer of adhesive at the double wall is modeled by solid elements. Symmetric boundary conditions are applied along all the edges of the foil, bottom areas are fixed and displacement load (crushing) is applied to an external rigid surface via a drop hammer which hits the top areas and moves with them. The main role of the top and bottom face plate is to contain the crushed honeycomb foil. In the actual mechanical test, a heavy steel hammer is used to crush the honeycomb. Material properties are given in Table 1. To replicate the actual test, the rigid surface is modeled using the rigid shell element and the mechanical properties are defined as that of steel but with a high fictitious density. AL5052 aluminum alloy with bilinear isotropic-hardening elastoplastic material model is used for the foil. Since the yield and ultimate strength of the AL5052 foil are very close, bilinear elastoplastic material model with very low tangent modulus is a reasonable approximation. The adhesive is modeled as perfectly plastic. Automatic single surface contact is applied to the model with sliding and sticking frictional coefficients equal to 0.2

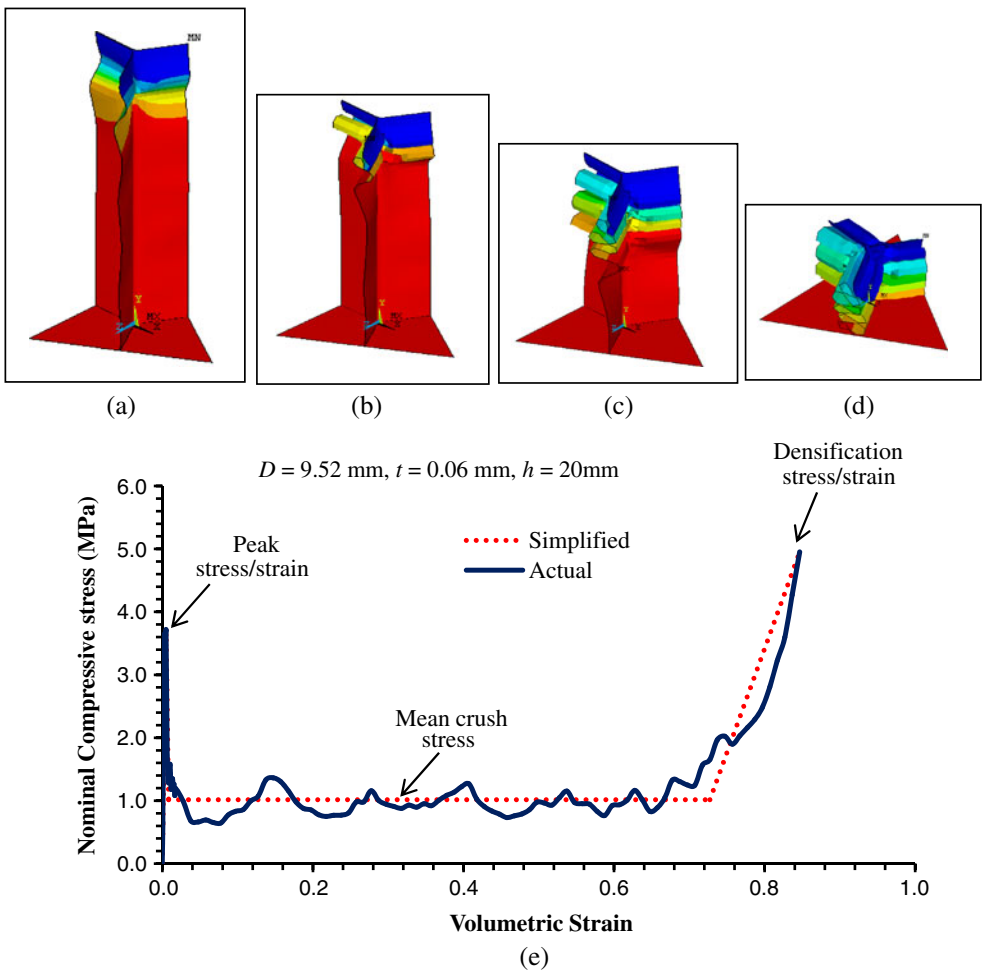

Fig. 2 Honeycomb core crushing (**a**)–(**d**) Different stages of honeycomb unit cell crushing and (**e**) obtained load curve and its different parameters

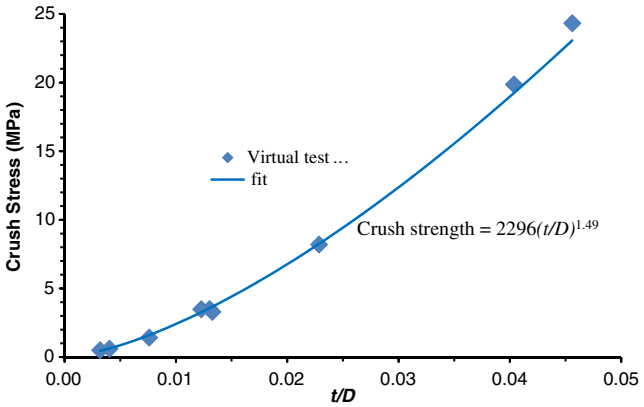

Fig. 3 Variation of crush strength with t/D obtained from virtual testing

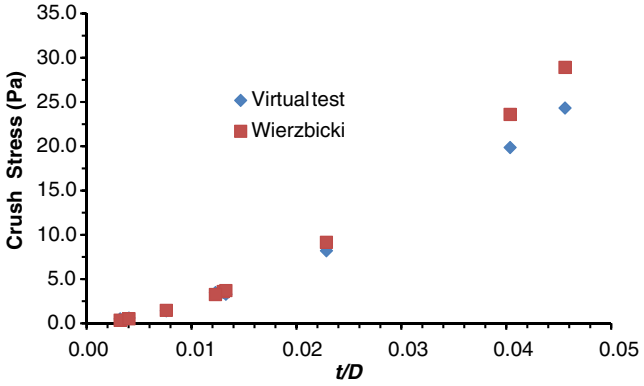

Fig. 4 Validation of the crush strength obtained from the virtual test

and 0.3, respectively. These mechanical properties of the foil and the adhesive, and friction coefficient values are obtained from the literature (Yamashita and Gotoh 2005). All the tests are carried out at a hammer speed of 80 mm/s along the depth of the honeycomb, which can be considered as quasi-static tests since impact tests involve very high hammer speeds in the order of m/s.

2.2 Geometrical parameters related to unit cell

The following parameters of the honeycomb cell geometry were considered: foil thickness t, cell size D which equals the distance between opposite walls of the honeycomb cell, and core depth, h. Preliminary FE runs show that the stress–strain or load curve does not show any visible change with core depth h (Zhang and Ashby 1992), provided that it is not too small so as not to allow folds to occur during crushing. Further the ratio t/D is the defining parameter that characterizes the load curve. This has also been reported in Wierzbicki (1983). The density is linearly proportional to t/D, as will be given below.

2.3 Nonlinear virtual testing and parametrization of the stress–strain curve

Figure 2 shows a typical crushing phenomenon and load curve obtained from the FE test. As the hammer travels, buckling (Yamashita and Gotoh 2005; Zhang and Ashby 1992) of the foil starts from near the impact edge and propagates downward. Compressive stress is obtained by dividing the reaction force experienced by the hammer by the triangular unit cell area, and volumetric strain is calculated from change in core depth divided by its original value. The core

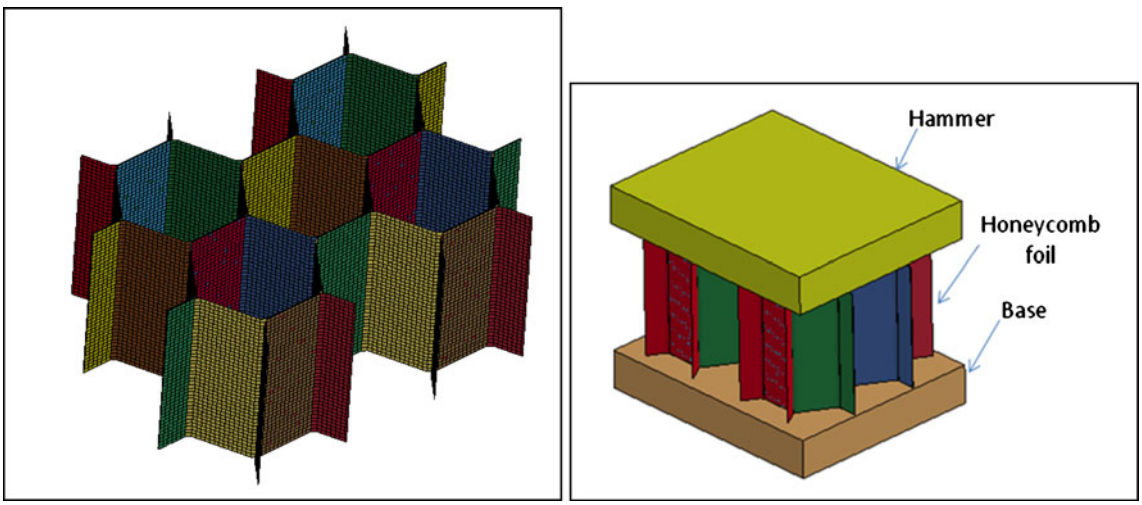

Fig. 5 Detailed model of test specimen

resists buckling until the peak stress point. Onset of buckling causes a sudden drop in the compressive stress (Fig. 2a). Compressive stress drops until the first folding of the cell wall is complete (Fig. 2b) and then stress increases. This goes on, although the peaks are very small in comparison to the first peak, until the whole core is folded. The crush strength (i.e. the plateau stress level) is the average of the oscillatory stress during the cyclic collapse of the foil. Once the entire core is folded, densification starts resulting in very high compressive stress. Large amount of energy gets dissipated through the plastic deformation of the cell wall at each folding. The energy absorbed per unit area of the core is essentially equal to the area under the load curve multiplied by core depth. Although sufficient care has been taken in approximating the load curve, it is not possible to define the crush start and end strain very accurately.

By repeated virtual tests for different values of t/D, and using curve fitting (Fig. 3 shows this for crush strength), we obtain the following equations that parameterize the load curve in terms of honeycomb geometry. Below, ρ_f = density of foil material in kg/m^3 and S_y = yield stress of the foil material (aluminum, here). Mass density refers to the mass per unit cell area and per unit depth. Yield stress and density refer to that of AL5052 material. Crush start and end strain do not change much with t/D and corresponding strain values are taken as 0.009 and 0.744 respectively. Final strain is fixed at 0.85.

$$\text{Mean crush stress (MPa)} = 2296\,(t/D)^{1.49}$$

$$\text{Peak strain} = 0.0626\,(t/D) + 0.0035$$

$$\text{Peak stress (MPa)} = 845.8\,(t/D) - 0.959$$

$$\text{Young's modulus} = \text{Peak stress/Peak strain}$$

$$\text{Crush start strain} = 0.009$$

$$\text{Crush end strain} = 0.744$$

$$\text{Densification strain} = 0.85$$

$$\text{Densification stress (MPa)} = 35592\,(t/D)^{1.69}$$

$$\text{Tensile stress cutoff (MPa)} = \frac{8S_y}{3}\,(t/D)$$

$$\text{Mass density}\left(\text{kg/m}^3\right) = \frac{8\rho_f}{3}\,(t/D) \qquad (1)$$

Relations in (1) provide a homogenized model for the honeycomb core.

2.4 Validation of the homogenized model

Several validation techniques are discussed here. Firstly, Wierzbicki (1983) showed that the mean crush strength may be given by

$$Mean\ crush\ strength = 16.565_y\left(t/D\right)^{5/3} \qquad (2)$$

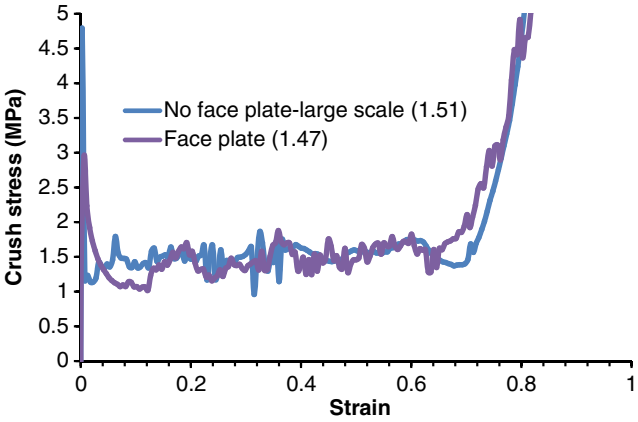

Fig. 6 Comparison of load curves from unit cell and detailed model on a virtual test specimen. Numbers in the parenthesis is the average crush strength

The analytically derived formula in (2) shows good agreement with the corresponding equation obtained from virtual testing in (1) as shown in Fig. 4. Secondly, the load curve obtained from the model in Fig. 1 is compared to that obtained from a detailed model of a test specimen (Fig. 5). The load curves match well (Fig. 6). Here, various boundary conditions have been virtually tested including random imperfections in geometry, all producing good agreement with the baseline test reported above.

Thirdly, since the homogenized model is based on crushing, and the blast panel is subject to both bending and crushing, validation via both bending and crushing virtual were performed. A 3-point bend test comparing the homogenized model above with a detailed virtual test specimen was carried out (Fig. 7). Provisions of ASTM standards D 7250 and C 393 are used (ASTM 2006a, b). For this test, $t/D = 0.00754$ is used. The response matches well for this bending application as well (Fig. 8). Comparison of a beam with span of beam perpendicular to the ribbon was also carried out with good agreement. Further, energy calculations were also in good agreement. Many details related

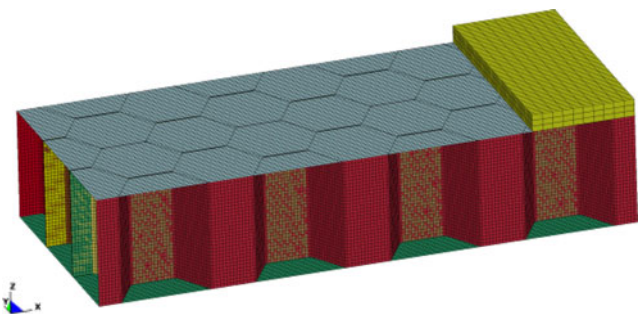

Fig. 7 Honeycomb ribbon orientation parallel to span of sandwich beam-detailed model

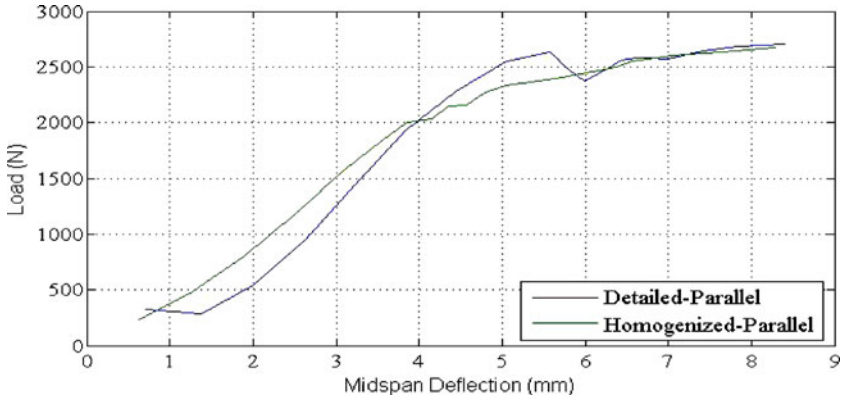

Fig. 8 Maximum deflection of the sandwich vs. contact load when honeycomb ribbon is parallel to the span of sandwich beam

to loading, boundary conditions and material properties in this beam test are omitted for brevity (Singh 2011), as the focus is on showing a process by which we can be confident of using the homogenized model for optimization.

3 Optimization problem formulation

Optimal design of a square honeycomb core sandwich panel subjected to air blast loading is considered (Fig. 9). The panel is freely suspended. The role of the stiffener at the top is to impose high inertia to the back face plate and hence the sandwich, permitting compression of the core. This set of boundary conditions are motivated by design problems in vehicle protection and approximate commonly used experimental fixtures. A study of different boundary conditions on monolithic plates, in contrast with sandwich panels as considered here, was previously conducted in Argod et al. (2010).

In general, design variables include thicknesses of face plates, core depth, core t/D or equivalently core density, and bulge magnitudes of the face plates (Fig. 10). Thus, $\mathbf{x} = \{t_b, t_f, h, t/D, s_b, s_f\}$.

Two separate objectives are considered for minimization: one is the peak displacement magnitude and the other is the rigid body acceleration, of the back face plate. Constraints are: limits on total mass and on plastic strain limit in the face plates, the latter to ensure structural integrity. Thus, we have the problem

$$\begin{array}{lll} \text{Minimize} & \max \delta_b & (\text{case}-1) \\ & \max \alpha_b & (\text{case}-2) \\ \text{subject to} & \varepsilon_{pj} \le \varepsilon_{pmax} & \text{for each element } j \text{ in the face plates} \\ & M \le M_{\max} & \text{mass limit} \\ & \mathbf{x}^{\mathrm{L}} \le \mathbf{x} \le \mathbf{x}^{\mathrm{U}} & \text{bounds on variables} \end{array} \tag{3}$$

In case-1, since the sandwich model is not constrained, the maximum Z-deflection of the back face plate is obtained by subtracting the rigid body displacement of the stiffener as $\delta_b = \delta_{Z\_\max} - \delta_{\text{stiffener}}$. Displacements along the x- and y- direction are not significant and are not considered. The displacement is a function of time, and the peak value is monitored. In case-2, the absolute maximum rigid body acceleration of back face plate along z-direction is considered. Like displacement, accelerations along the x- and y-direction are not significant. Rigid body acceleration refers

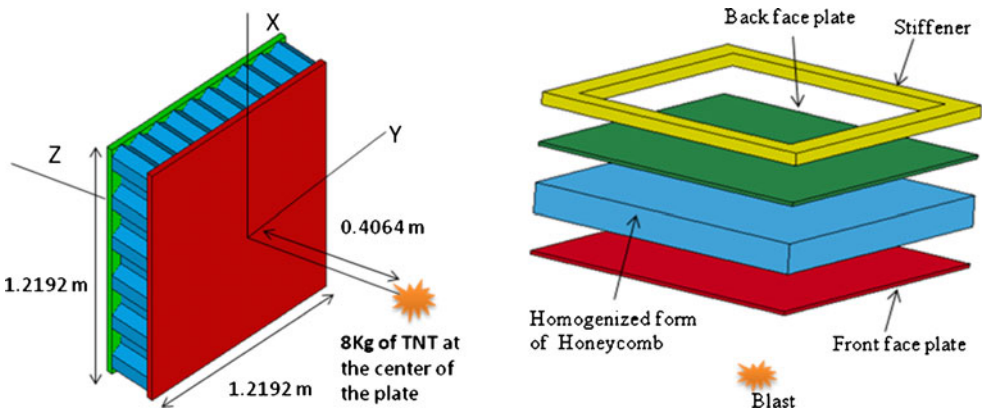

(a) (b)

Fig. 9 (**a**) Honeycomb sandwich panel (**b**) Exploded view of the honeycomb core sandwich model used for optimization study

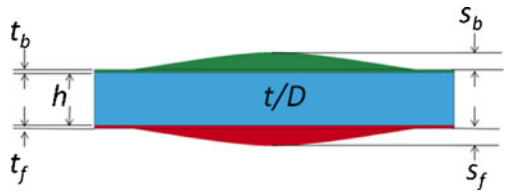

Fig. 10 Optimization parameters for the sandwich optimization

to net force divided by net mass. The plastic strains in the face plates increase with simulation time until a plateau is reached and this saturated or maximum value is considered. The maximum value of the all elements in the face plates is monitored. The mass M is the sum of the mass of the front and back face plates and of the core as $M = M_f + M_b + M_c$. Mass of the stiffener remains constant during optimization and is not included in M.

Optimization is carried out in the following sequence: (I) optimization for case-1 considering only $\{t_b,\ t_f,\ h,\ t/D\}$ as variables, (II) optimization for case-1 considering all six variables $\{t_b, t_f, h, t/D, s_b, s_f\}$, and (III) optimization for case-2 considering only $\{t_b, t_f, h, t/D\}$.

For brevity in the figure captions, we refer to $\{t_b,\ t_f,\ h, t/D\}$-optimized panel as 'size-optimized panel', and $\{t_b,\ t_f,\ h,\ t/D,\ s_b,\ s_f\}$-optimized panel as, 'size+shape optimized panel'.The variable t/D is a parameter that defines the stress–strain curve which is input into LS-DYNA. The remaining five variables $\{t_b,\ t_f,\ h,\ s_b,\ s_f\}$ require a change in the coordinates of the nodes in the 3D finite element model. That is, they affect the *shape* of the structure. The key equation to implement shape optimization is (Belegundu and Rajan 1988)

$$\mathbf{G}\,(\mathbf{x}) = \mathbf{G}_{\text{original}} + \sum_{i=1}^{N_{dv}} x_i \mathbf{q}^i \tag{4}$$

where $\mathbf{G}$ is a grid point coordinates vector, representing x-, y-, z- coordinates of all nodes in the model. Each x_k represents the amplitude of a 'permissible shape change vector' or what is commonly called a 'velocity field' vector $\mathbf{q}^k$. Velocity fields have nothing to do with actual velocities of the model under loading. Vectors $\{\mathbf{q}^k\}$ are generated just once in the optimization procedure. $\mathbf{G}_{\text{original}}$ is the current (flat) shape. Visualization of a $\{\mathbf{q}^i\}$ is identical to visualization of a displacement field in finite elements: $\{\mathbf{q}^k\}$ is multiplied by a magnification scalar and added to the current grid to obtain a displaced grid, except that here the displaced grid represents a new shape and is called a *basis shape*.

Velocity fields associated with variables $t_b,\ t_f,\ h$ are straightforward: nodes are moved in the $+/-$ z-direction, maintaining equal spacing, to result in the desired thicknesses. For variables s_b and s_f, which are the amplitudes of basis shapes that correspond to *bulges* in the face plates as shown in Fig. 10, a procedure is needed to generate $\mathbf{q}^i$. The velocity fields $\mathbf{q}^i$ are generated here by first applying a dummy load on each of the plate surfaces and using analytical expressions in Timoshenko and Woinowsky-Krieger (1959), Eq. 145, page 142, to obtain the corresponding nodal displacements on all nodes on the surface. Then, equal spacing in the z-direction is used to complete the definition of $\mathbf{q}^i$. A square portion (1.016 m $\times$ 1.016 m) at the center of the face plates is taken as the domain for applying velocity fields. Asymmetric shape variations are not necessary in this problem owing to centrally located charge. Lower bounds s_b and s_f are zero implying that only convex (outward) bulges are allowed for shape changes, as this has found to be beneficial in deflecting the waves in the monolithic plate (Argod et al. 2010; Belegundu et al. 2008).

As variables $\mathbf{x} = \{t_b,\ t_f,\ h,\ t/D,\ s_b,\ s_f\}$ are changed for each sampling point, the grid point coordinates $\mathbf{G}$, the load curve from (1), and thickness values are updated, an LS-DYNA input file is then written, and an analysis is carried out to evaluate the various functions in the optimization problem. The process is schematically given as:

> Use current values of $\{t_b, t_f, h, s_b, s_f\}$ at sampling point $\mathbf{x}^k$, construct $\mathbf{G}$ using $\{\mathbf{q}^i\}$; from current value of $\{t/D\}$, construct the stress–strain curve data using (1) → Write input file and perform LS-DYNA analysis → Evaluate objective and constraint functions → Create response equations → Run optimizer

The DOE response surface method is used to solve this problem, implemented using Design Expert, a commercially available software. Using the response equations, optimization is carried out by *fmincon*, a gradient based optimizer in MATLAB optimization toolbox. Central composite face centered (CCF) method is adopted to create design points. It uses three levels for each factor. Lower design limits are decided in such a way that FE evaluation is feasible at all sampling points and to avoid high aspect ratios in the hexahedral elements. Also, appropriate upper

Table 2 Design limits for $\{t_b, t_f, h, t/D\}$-optimization, min. δ_b

Design limits	Lower limit	Upper limit
Front face plate thickness (mm), t_f	4.4	18
Core depth (mm), h	280	500
Foil thickness/cell size, t/D	0.018	0.046
Back face plate thickness (mm), t_b	4.4	10

Table 3 Optimization results for $\{t_b, t_f, h, t/D\}$-optimization with varying mass limits, min. δ_b (units: mm)

Sandwich mass (kg)	Optimized parameters					ε_{pmax}
	t_f	h	t_b	(t/D)	δ_b (Obj)	
130	8.07	300.6	4.4	0.0252	24.3	0.0384
140	7.90	359.9	4.4	0.0238	19.96	0.0373
150	7.55	401.6	4.4	0.0240	16.92	0.033
160	8.4	390.2	4.4	0.0263	14.65	0.023
170	9.12	388	4.4	0.0282	12.43	0.017

design limits are taken so that better response fit is possible and at the same time giving more design space to the optimizer to find the minima. Design limits for the different cases are given in Tables 2, 3 and 4 below. Some results have been cross-checked by using the differential evolution (DE) technique which is computationally more expensive.

4 FE modeling using LS-DYNA

In this study, aluminum AL5052 is considered for the entire sandwich such that results can be easily compared with AL5052 monolithic plate considered earlier (Argod et al. 2010; Belegundu et al. 2008). In the monolithic plate problem, various boundary conditions were considered giving similar optimum shapes (Argod et al. 2010). The model is free to move in space, which approximates to some extent commonly used experimental fixtures. As a consequence of this, the back face plate is not restrained and can deform freely without creating unrealistically high plastic strain. The role of the stiffener at the top is to impose high inertia to the back face plate and hence the sandwich, permitting compression of the core. Mass of the stiffener is 1,850 kg. High fictitious density is defined for the stiffener. The contacts between the face plate and the core, and between the back face plate and the stiffener are defined using *CONTACT features and *TIED_SURFACE_TO_SURFACE_ID card. After a mesh convergence study a 38 × 38 × 2 and 28 × 28 × 3 element mesh is taken in x-y plane for the face plates and the core, respectively. The *MAT_PLASTIC_KINEMATIC material model is used for the face plates and *MAT_CRUSHABLE_FOAM material model is used for the core. Material properties used for the face plate are same as that of the foil used for honeycomb virtual testing (Table 1). The mechanical properties of the core are defined in (1), which are functions of t/D. Poisson's ratio is taken as zero for the core. The *LOAD_BLAST input parameters used are equivalent TNT mass (8 kg), type of blast (air blast-spherical charge), load curve, charge location (0, 0, −0.4064 m). The exposed bottom surface of the plate is defined as the area on which blast load applied. A low value of damping ≈ 1e-9 and a reduced tssfac help in smoother convergence in LS-DYNA.

5 Optimization results

Results are discussed here for different mass limits for the sandwich, while detailed response is given for the 150 kg mass limit. The optimization study is carried out for a fixed amount of charge, viz. 8 kg TNT. When the DOE response surface optimizer provides an optimum set of design variables, LS-DYNA is executed, and the resulting response values are used in the tables below.

5.1 Optimization results for minimum backface displacement, δ_b

We note that δ_b refers to the peak in the displacement-time response of the backface relative to the stiffener. Table 5 shows the $\{t_b, t_f, h, t/D\}$-optimized sandwich panel parameters for different mass limits. The ε_{pmax} is always at

Table 4 Design limits for $\{t_b, t_f, h, t/D, s_b, s_f\}$-optimization, min. δ_b

Design limits	Lower limit	Upper limit
Front face plate thickness (mm), t_f	4.4	10
Core depth (mm), h	150	500
Foil thickness/cell size, t/D	0.018	0.046
Back face plate thickness (mm), t_b	4.4	10
Front face plate bulge (mm), s_f	10	100
Back face plate bulge (mm), s_b	0	100

Table 5 Optimization results for $\{t_b, t_f, h, t/D, s_b, s_f\}$-optimization with varying mass limits, min. δ_b (units: mm)

Sandwich mass (kg)	Optimized parameters							ε_{pmax}
	t_f	h	t_b	(t/D)	s_f	s_b	δ_b (Obj)	
130	4.4	150	4.4	0.0364	42.41	0	20.76	0.031
140	4.4	150	4.4	0.0371	52.69	0	17.04	0.020
150	4.4	150	4.4	0.0377	62.96	0	14.4	0.014
160	4.4	150	4.4	0.0384	73.24	0	12.25	0.012
170	4.4	150	4.4	0.039	83.52	0	10.73	0.001

Table 6 Design limits for $\{t_b, t_f, h, t/D\}$-optimization, min. a_b

Design limits	Lower limit	Upper limit
Front face plate thickness (mm), t_f	15	25
Core depth (mm), h	120	400
Foil thickness/cell size, t/D	0.00754	0.025
Back face plate thickness (mm), t_b	8	25

the center of the front face plate. With increase in mass, δ_b decreases. The optimizer produces thicker and denser (higher t/D) core. Mass is always active and the plastic strain is active only for 130 kg and 140 kg.

Table 6 shows the $\{t_b, t_f, h, t/D, s_b, s_f\}$-optimized sandwich panel parameters for different mass limits. The ε_{pmax} is always in the back face plate. With increase in mass, δ_b decreases. The optimizer produces a denser or higher t/D core. The t_b is always at lower limit (4.4 mm) for the reason mentioned in Section 6. The t_f is always at lower limit (4.4 mm) as the front face plate thickness re-emerges in the bulge. The bulge also reduces the effective blast load on the panel by deflecting the blast. The bulge also provides higher stiffness to the panel, compensating for the loss in stiffness due to lower core depth. With increase in mass, t/D and s_f increase consistently. Mass is always active and the plastic strain is always inactive.

Now, focusing on the 150 kg mass limit, Fig. 11 shows the performance of the optimized sandwich panel and how it compares with an all-aluminum monolithic plate. A non-optimized uniformly thick aluminum panel is also included in the comparison for reference purposes. The corresponding backface deflection-time responses are shown in Fig. 12a, plastic strains in Fig. 12b and Z-momentum in Fig. 12c. Compared to the uniformly thick aluminum panel, the sandwich panel shows significant reduction. Shape optimization of the sandwich adds to this improvement. However, a shape-optimized all-aluminum panel scored a victory as compared to the sandwich (11.5 mm to 14.4 mm deflection). A physical explanation for this is given subsequently. In the sandwich, the mass fraction in the front face plate, core and the back face plate are 0.20, 0. 68 and 0.12, respectively, for the $\{t_b, t_f, h, t/D\}$-optimized panel and 0.48, 0.40 and 0.12, respectively, for the $\{t_b, t_f, h, t/D, s_b, s_f\}$, optimized panel.

6 Mechanism causing the improvement in backface deflection

In the $\{t_b, t_f, h, t/D\}$-optimized panel, the optimizer has chosen a larger core depth which increases the overall stiffness of the sandwich and lowers δ_b. The t_b is always at lower limit (4.4 mm) as it is sufficient to keep ε_{pmax} below the strain limit (0.038). The t_f is decided based on three things, viz. to keep ε_{pmax} below the strain limit, to provide sufficient stiffness for the front face plate to transfer the blast pressure load to a larger area of the core, and to reduce local concave deformation of the front face plate which will increase the impulse.

Compared to the $\{t_b, t_f, h, t/D\}$-optimized panel above, the $\{t_b, t_f, h, t/D, s_b, s_f\}$-optimized panel has further reduced the deflection by 14.9 %. This may be attributed to the following mechanisms. A lesser core depth has been produced but with a bulge in the front face plate. The core is denser. The bulge deflects the blast wave and reduces

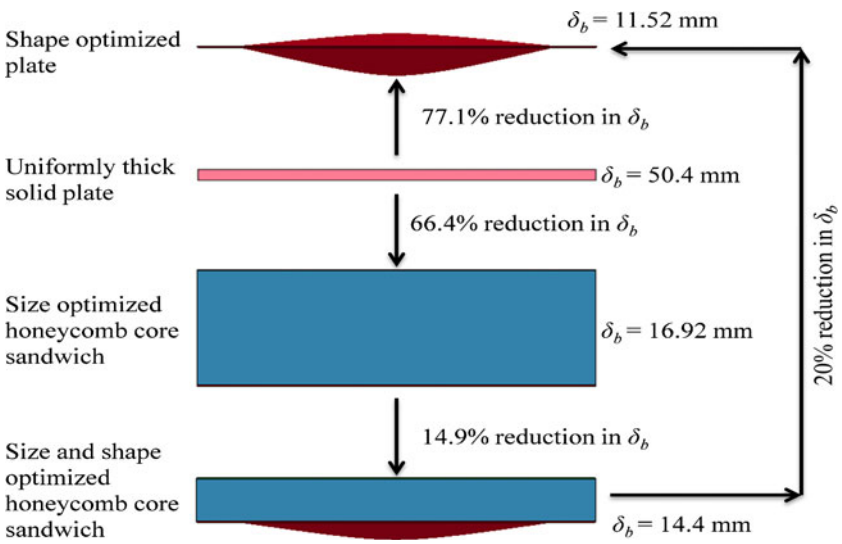

Fig. 11 Optimized sandwich panel and shape optimized monolithic plate of 150 kg mass for minimizing δ_b (stiffener not shown)

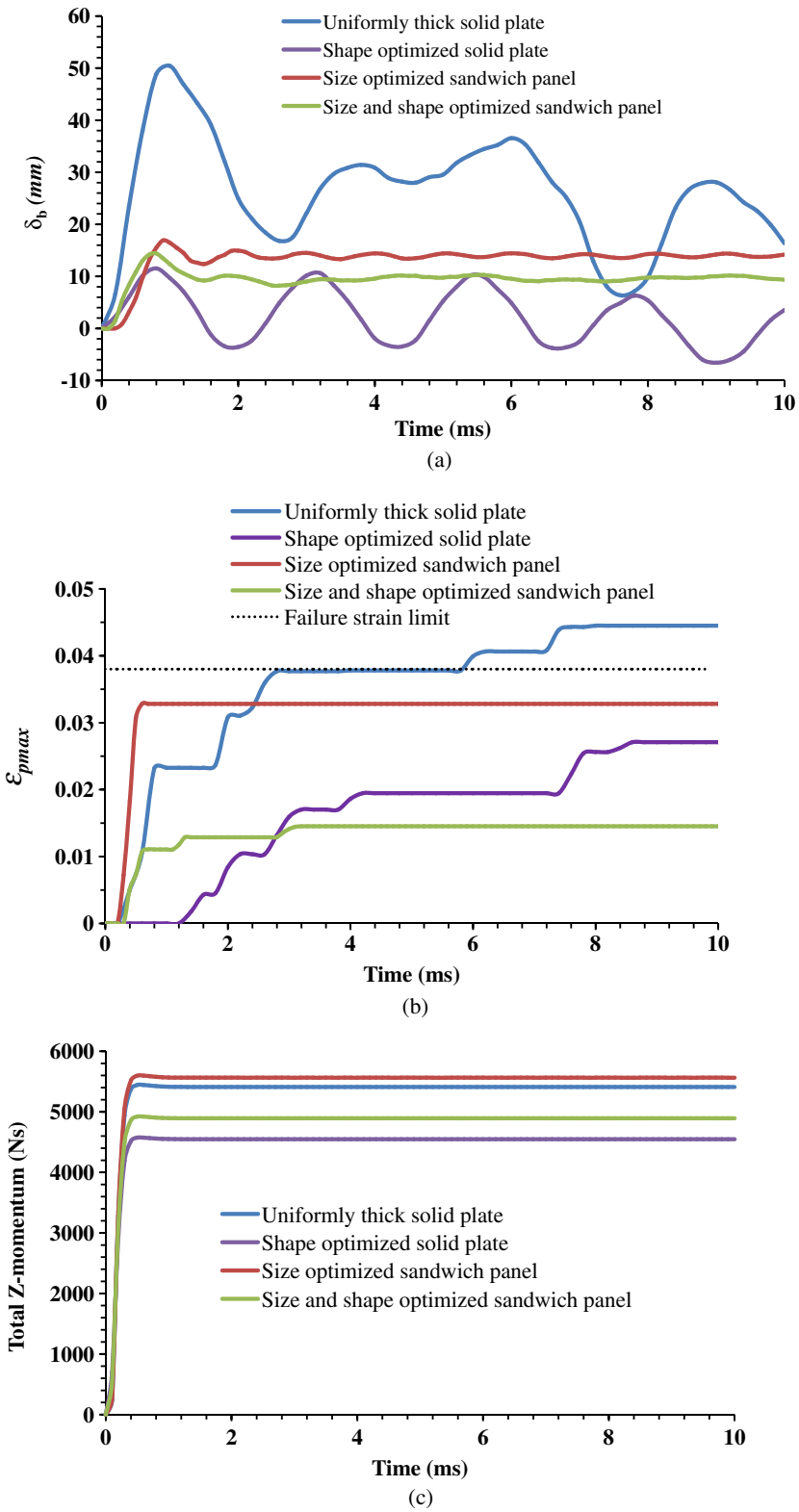

Fig. 12 Comparison for minimum δ_b for 150 kg mass limit: (**a**) δ_b, (**b**) ε_{pmax} and (**c**) total Z-momentum. Note: by solid plate is meant a monolithic all-metal plate

the impulse imparted to the structure, and it also increases the moment of inertia of the sandwich at its center where blast load is maximum. The bulge also makes the front face plate stiffer, which helps to transfer the blast load to a large area of the core thereby reducing local deformation at the center.

Table 7 Optimization results for $\{t_b, t_f, h, t/D\}$-optimization with varying mass limits, min. a_b (units: mm, m/s^2)

Sandwich mass (kg)	Optimized parameters					ε_{pmax}
	t_f	h	t_b	(t/D)	a_b (Obj)	
130	17.94	194.93	10.77	0.00754	2.77×10^4	0.0355 (f)
140	17.79	196.84	13.4	0.00754	2.22×10^4	0.0360 (f)
150	17.63	199.22	16.02	0.00754	1.84×10^4	0.0371 (f)
160	17.45	202.16	18.64	0.00754	1.57×10^4	0.0388 (f)
170	17.45	205.2	21.1	0.00754	1.37×10^4	0.0388 (f)

In the all-aluminum monolithic plate, more mass is available to go in terms of bulge, whereas in the sandwich, mass is distributed between face plates and core. Higher the bulge height towards the blast, greater is the reduction in impulse and hence greater the reduction in backface deflection. This aspect and higher rigidity makes the monolithic plate slightly better than the sandwich panel as shown in Fig. 11a.

6.1 Optimization results for minimum backface acceleration, a_b

Table 7 summarizes the $\{t_b, t_f, h, t/D\}$-optimized results for different mass of the sandwich. With increase in mass, a_b decreases. It shows that both h and t_b increases with sandwich mass, but t_f does not vary much. The core density (proportional to t/D) always remains at the lower bound. The ε_{pmax} is very close to the limiting value of 0.038 for all the mass limits. It can be observed that with increase in sandwich mass, the optimizer adds mass more to the back face plate than to the core; a_b not only depends upon the force transmitted to the back face plate but also on the back face plate mass (Main and Gazonas 2008; Karagiozova et al. 2009).

Focusing on the 150 kg mass limit, Fig. 13 shows the performance of the optimized sandwich panel and how it compares with an all-aluminum monolithic plate. The corresponding acceleration-time responses are shown in Fig. 14a. $\{t_b, t_f, h, t/D\}$-optimized sandwich panel results in 84 % reduction in a_b compared to a uniformly thick monolithic plate of equal mass. The location of the ε_{pmax} is at the center of the front face plate.

Now, comparing the optimized sandwich to an optimized all-aluminum monolithic panel, the sandwich scores a clear victory (compare 1.84×10^4 to 8.88×10^4 m/s^2). Recall that the victor was reversed for δ_b minimization. The monolithic plate has no mechanism for energy absorption. The mass fraction in the front face plate, core and the back face plate are 0.47, 0.11 and 0.42 respectively.

7 Mechanism causing the improvement in backface acceleration

A paper by Avalle et al. (2001) explains the relation between energy absorption and transmitted force. We note that a_b is a direct measure of the transmitted force, and that core density ρ and t/D are linearly related. In Fig. 15, the area under the three curves $\int \sigma \, d\varepsilon$ are the same. The area represents energy per unit volume, and σ_b denotes the corresponding stress value, which is here the compressive stress in the core elements in contact with the back face plate. For low density core ρ_1, the deformation is high and the stress–strain state is in the densification zone with high stress. For high density core ρ_3, the energy is absorbed with low deformation and high stress. The medium density foam ρ_2 is optimum as σ_b is lowest. In fact, an efficiency index has been defined in (Avalle et al. 2001) as

$$\eta = \frac{\int \sigma \, d\varepsilon}{\sigma_b} \tag{5}$$

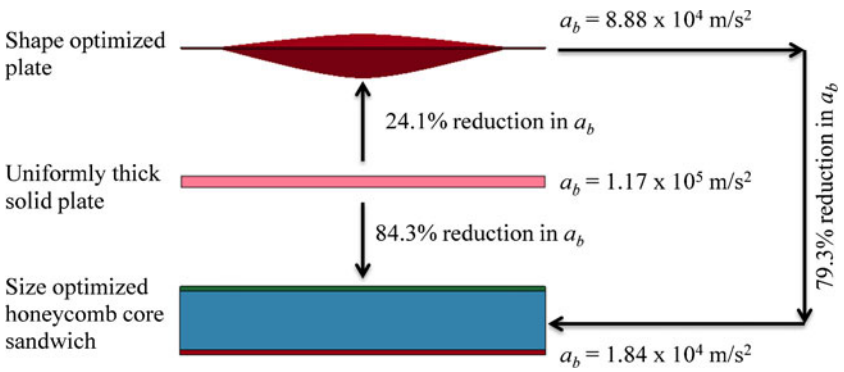

Fig. 13 Optimized sandwich panel and shape optimized monolithic plate of 150 kg mass for minimizing a_b (stiffener not shown)

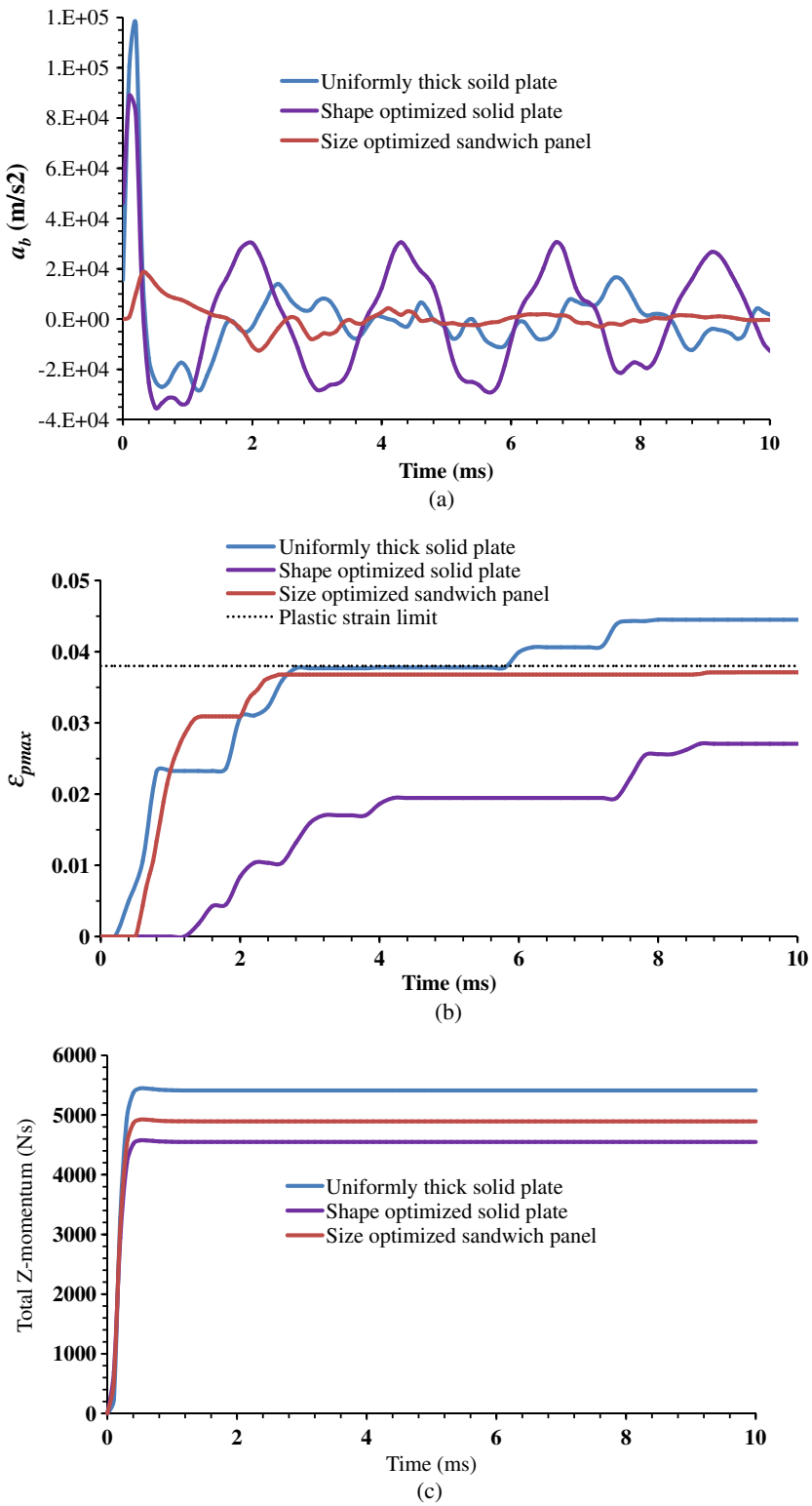

Fig. 14 Comparison for minimum a_b for 150 kg mass limit: (**a**) a_b, (**b**) ε_{pmax} and (**c**) total Z-momentum

Higher efficiency implies that the core absorbs a given amount of energy with lesser transmitted force. A look at the results show that optimization has exploited this physics: t/D and core depth have been adjusted so that even though the maximum strain in front face elements have gone to the densification region (strain $>$ 0.744), the strain in the

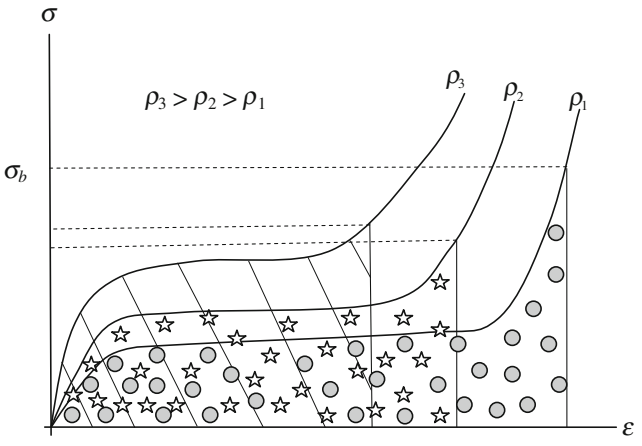

Fig. 15 Stress (at the backface) for different density foams corresponding to same energy absorption

backface elements are well within the crushing zone avoiding complete densification. The t/D has been pushed to its lower bound. Further, a comparison of η between the optimized results for a_b vs. δ_b minimization (Table 8) clearly shows that the optimizer has done its task: when the objective is a_b, a more efficient core is designed. Of course, optimization also adjusts the mass distribution between face plates and core, subject to constraints on sandwich mass, plastic strain in plates and lower bounds on t/D.

8 Conclusions

A process for optimizing sandwich panels to mitigate blast loading is presented. While honeycomb core has been used in the study, the process is also applicable to other types of cellular core. Two independent design objectives, backface deflection of the plate and backface acceleration are minimized, subject to mass and plastic strain constraints. The optimization is carried out using DOE response surface methodology. LS-DYNA is used for finite element simulations. Virtual testing is used to develop a homogenized model for the stress–strain curve of the honeycomb core, and this model has been validated by comparison to existing results as well as to detailed FE model results.

The mechanism of lowering the backface deflection is by increasing front face plate thickness which effectively distributes the blast load to a larger area of the core and avoids increase in impulse stemming from local concave deformation of the front face plate. Further, core depth is increased which increases panel stiffness. In the sandwich, the mass fraction in the front face plate, core and the back face plate are 0.20, 0. 68 and 0.12, respectively, for the $\{t_b, t_f, h, t/D\}$-optimized panel. Interestingly, for the same mass, the shape-optimized monolithic panel is more effective than the optimized honeycomb core sandwich panel (11.5 mm vs. 14.4 mm). In the all-aluminum monolithic plate, more mass is available to go in terms of bulge, whereas in the sandwich, mass is distributed between face plates and core. Higher the bulge height towards the blast, greater is the reduction in impulse and hence greater the reduction in backface deflection. This aspect and higher rigidity makes the monolithic plate slightly better than the sandwich panel as shown in Fig. 11a.

Considering acceleration minimization, results produce a stiffer front face plate, which helps to distribute the crushing load to a wider region of the core, and a soft core by reducing t/D to its minimum value. The mechanism of lowering the backface acceleration is by absorbing energy with low transmitted stress. In this case, honeycomb core sandwich panel proves to be significantly more effective than an optimized monolithic panel (1.84e4 m/s^2 vs. 8.88e4 m/s^2). With increase in sandwich mass, the optimizer adds mass more to the back face plate rather than the core; acceleration not only depends upon the force transmitted to the back face plate but also on the back face plate mass. In the sandwich, the mass fraction in the front face plate, core and the back face plate are 0.47, 0. 11 and 0.42, respectively.

As noted earlier, Yen et al. (2005) had carried out an experimental and computational study, and concluded that significant reduction in maximum stress amplitude propagating within the core can be achieved by suitable selection of honeycomb material with proper crush strength. This observation has been borne out by the results here, as optimization with LS-DYNA achieves a proper balance, accounting for different interacting physics. A general and efficient design process has been presented.

Fracture of the face plates themselves has been avoided by imposing a limit on maximum plastic strain during optimization. However, fracture causing debonding between the core and the face plates has not been considered in this study. Finally, the work here can be extended to include strain rate sensitivity in the homogenization model.

Table 8 Comparison of honeycomb core energy absorption efficiency

Case	t/D	$\int \sigma \, d\varepsilon$ (Pa)	σ_b (average) (Pa)	η
acceleration_ min ($a_b^* = 1.84 \times 10^4$ ms^{-2})	0.00754	702377.6	1.58×10^6	44.5 %
deflection_min ($a_b^* = 7.25 \times 10^4$ ms^{-2})	0.024	569514.2	5.59×10^6	10.2 %

Acknowledgments This material is based upon work partly supported by the Army Research Office, Proposal Number 50490-EG, monitored by Dr. Bruce LaMattina. Partial financial and computational support from the High Performance Computing Group at Penn State under Mr. Vijay Agarwala is gratefully acknowledged.

References

Argod V, Nayak SK, Singh AK, Belegundu AD (2010) Shape optimization of solid isotropic plates to mitigate the effects of air blast loading. Mech Base Des Struct Mach 38:362–371

ASTM D 7250/D 7250M-06 (2006a) Standard practice for determining sandwich beam flexural and shear stiffness

ASTM C 393/C 393M-06 (2006b) Standard test method for core shear properties of sandwich constructions by beam flexure

Avalle M, Belingardi G, Montanini R (2001) Characterization of polymeric structural foams under compressive impact loading by means of energy-absorption diagram. Int J Impact Eng 25: 455–472

Belegundu AD, Rajan SD (1988) A shape optimization approach based on natural design variables and shape functions. J Comput Methods Appl Mech Eng 66:87–106

Belegundu AD, Argod V, Rajan SD, Krishnan K (2008) Shape optimization of panels subject to blast loading modeled with LS-DYNA. In: 49th AIAA/ASME/ASCE/AHS/ASC structures, structural dynamics, and materials conference, paper AIAA 2008–2285, Schaumburg, IL

Chi Y, Langdon GS, Nurick GN (2010) The influence of core height and face plate thickness on the response of honeycomb sandwich panels subjected to blast loading. Mater Des 31:1887–1899

Fleck NA, Deshpande VS (2004) The resistance of clamped sandwich beams to shock loading. ASME J Appl Mech 71:386–401

Hanssen AG, Enstock L, Langseth M (2002) Close-range blast loading of aluminium foam panels. Int J Impact Eng 27:593–618

Karagiozova D, Nurick GN, Langdon GS (2009) Behaviour of sandwich panels subject to intense air blasts-parts 2: numerical simulation. Compos Struct 91:442–450

Main JA, Gazonas GA (2008) Uniaxial crushing of sandwich plates under air blast: influence of mass distribution. Int J Solid Struct 45:2297–2321

Singh AK (2011) MS thesis. Department of Mechanical and Nuclear Engineering, The Pennsylvania State University, University Park, PA 16802

Timoshenko SP, Woinowsky-Krieger S (1959) Theory of plates and shells. Engineering societies monographs, 2nd edn. McGraw-Hill, New York

Wierzbicki T (1983) Crushing analysis of metal honeycombs. Int J Impact Eng 1(2):157–174

Wu E, Jiang W-S (1997) Axial crushing of metallic honeycomb. Int J Impact Eng 19:439–456

Xue Z, Hutchinson JW (2004) A comparative study of impulse-resistant metal sandwich plates. Int J Impact Eng 30:1283–1305

Yamashita M, Gotoh M (2005) Impact behavior of honeycomb structures with various cell specifications - numerical simulation and experiment. Int J Impact Eng 32:618–630

Yen CF, Skaggs R, Cheeseman BA (2005) Modeling of shock mitigation sandwich structures for blast protection. In: The 3rd first international conference on structural stability and dynamics, Kissimmee, Florida, 19–22 June 2005

Zhang J, Ashby MF (1992) Buckling of honeycombs under in-plane biaxial stress. Int J Mech Sci 34:491–509

Zhu F, Zhao L, Lu G, Wang Z (2008) Deformation and failure of blast-loaded metallic sandwich panels-experimental investigations. Int J Impact Eng 35:937–951

Zhu F, Wang Z, Lu G, Zhao L (2009) Analytical investigation and optimal design of sandwich panels subjected to shock loading. Mater Des 30:91–100